BIOCHEMISTRY
including biophysical chemistry & molecular biology

Article

pubs.acs.org/biochemistry

A Copper−Methionine Interaction Controls the pH-Dependent Activation of Peptidylglycine Monooxygenase

Andrew T. Bauman,[†] Brenda A. Broers, Chelsey D. Kline, and Ninian J. Blackburn*

Institute of Environmental Health, Oregon Health and Sciences University, Beaverton, Oregon 97006, United States

Supporting Information

ABSTRACT: The pH dependence of native peptidylglycine monooxygenase (PHM) and its M314H variant has been studied in detail. For wild-type (WT) PHM, the intensity of the Cu−S interaction visible in the Cu(I) extended X-ray absorption fine structure (EXAFS) data is inversely proportional to catalytic activity over the pH range of 3−8. A previous model based on more limited data was interpreted in terms of two protein conformations involving an inactive Met-on form and an active flexible Met-off form [Bauman, A. T., et al. (2006) *Biochemistry* 45, 11140−11150] that derived its catalytic activity from the ability to couple into vibrational modes critical for proton tunneling. The new studies comparing the WT and M314H variant have led to the evolution of this model, in which the Met-on form has been found to be derived from coordination of an additional Met residue, rather than a more rigid conformer of M314 as previously proposed. The catalytic activity of the mutant decreased by 96% because of effects on both k_{cat} and K_M, but it displayed the same activity−pH profile with a maximum around pH 6. At pH 8, the reduced Cu(I) form gave spectra that could be simulated by replacement of the Cu_M Cu−S(Met) interaction with a Cu−N/O interaction, but the data did not unambiguously assign the ligand to the imidazole side chain of H314. At pH 3.5, the EXAFS still showed the presence of a strong Cu−S interaction, establishing that the Met-on form observed at low pH in WT cannot be due to a strengthening of the Cu_M−methionine interaction but must arise from a different Cu−S interaction. Therefore, lowering the pH causes a conformational change at one of the Cu centers that brings a new S donor residue into a favorable orientation for coordination to copper and generates an inactive form. Cys coordination is unlikely because all Cys residues in PHM are engaged in disulfide cross-links. Sequence comparison with the PHM homologues tyramine β-monooxygenase and dopamine β-monooxygenase suggests that M109 (adjacent to H site ligands H107 and H108) is the most likely candidate. A model is presented in which H108 is protonated with a pK_a of 4.6 to generate the inactive low-pH form with Cu_H coordinated by M109, H107, and H172.

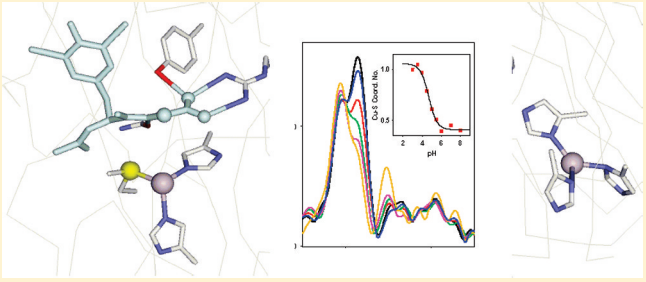

Peptidylglycine monooxygenase (PHM) catalyzes the first step in the amidation of neuropeptide hormones, converting the glycine-extended propeptide to its α-hydroxyglcine intermediate.[1] The catalytic core (residues 42−356) termed PHMcc is homologous to that of other copper monooxygenases involved in neurotransmitter biosynthesis such as dopamine β-monooxygenase (DBM)[2] and tyramine β-monooxygenase (TBM).[3] Spectroscopic studies have established structural similarities between their active sites,[4−8] but PHMcc is the only member of the group for which crystal structures are available.[9−12] Unlike the coupled binuclear centers common to hemocyanins, tyrosinases, catechol oxidases,[13−16] and oxygen-activating dicopper model complexes,[17] the copper centers in PHM are mononuclear and separated by 11 Å of a solvent-filled channel. The Cu_M center is coordinated by two histidines and a methionine, while the Cu_H center is coordinated to three histidine residues (Figure 1).

The detailed mechanism of substrate hydroxylation has been the subject of much debate. It is generally accepted that the enzyme cycles through a reductive phase in which the two copper centers are reduced to Cu(I) and an oxidative phase in which O_2 is activated and subsequently hydroxylates the substrate. A structure of the reduced enzyme cocrystallized with a slow substrate has revealed the presence of a dioxygen molecule bound at the Cu_M center, the bond length of which is consistent with a Cu(II)−superoxo species. A superoxo intermediate is supported by other biochemical[18,19] and theoretical[15,20] studies that implicate Cu(II)-$O_2^{\bullet-}$ as the reactive oxygen species. It has been further suggested that the large spatial separation of the Cu centers in PHM prevents formation of the peroxide and thus allows the potent electrophilic reactivity of the mononuclear Cu(II)−superoxo species to be fully expressed in the form of abstraction of H atoms from the substrate[15,18,20] to form a mononuclear hydroperoxo species at Cu_M. Subsequent steps in the reaction pathway are less clear, and alternate mechanisms that involve long-range transfer of an electron from Cu_H either before[18] or

Received: August 1, 2011
Revised: November 7, 2011
Published: November 14, 2011

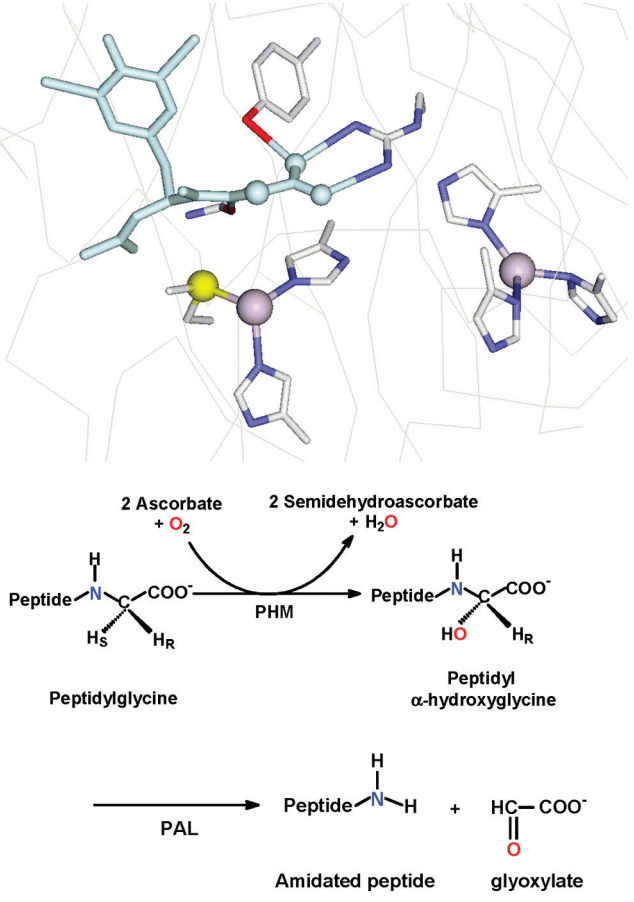

Figure 1. View of the active site of PHM (top) showing the Cu_H center (right) coordinated to three histidines and the Cu_M center (left) coordinated to two histidines and a methionine. A substrate molecule (di-iodo-YG) is bound in the site close to the M center (taken from PDB entry 1OPM). Reactions catalyzed by the PHM and PAL domains of peptidylglycine α-amidating lyase (PAM) (bottom).

after[20] the transfer of an OH group to the substrate radical to form product have been proposed.[17]

Early site-directed mutagenic studies of PHMcc M314X substitutions reported undetectable catalytic activity in the Ile, His, Asp, and Cys variants,[21,22] while more recent mutagenic analysis of the homologous Met ligand in TBM (M471) showed similarly low or undetectable activity for His, Asp, and Cys variants.[4] These studies established an essential role for M314 in PHM catalysis. Extensive characterization of the Cu−S bond by EXAFS[5−7,23,24] led to the finding that the interaction was unusually weak at pH values at or above the pH optimum (5.8) but became much more intense at lower pH values. This led to the suggestion that the dynamics of the Cu−S(Met) interaction were controlling catalytic activity via a "Met-on" (inactive) to "Met-off" (active) structural transition.[24]

In this work, we explore further the relationship between catalytic activity and the Cu(I)−methionine interactions as a function of pH. Using a complex buffer system containing formate, MES, HEPES, and CHES, we have determined the complete pH−activity profile between pH 3 and 8 and correlated this with changes in the strength or shell occupancy of the Cu−S interaction in the EXAFS. These results suggest that the strengthening of the Cu−S interaction is due to coordination of an additional S ligand at low pH mediated by a conformational change at one of the Cu centers, which brings a new S donor residue into a favorable orientation for coordination to copper, thereby generating the inactive form. Cys coordination is unlikely because all Cys residues in PHM are engaged in disulfide cross-links. Sequence comparison with the PHM homologues TBM and DBM suggests that M109 (adjacent to H site ligands H107 and H108) is the most likely candidate. A model is presented in which H108 is protonated with a pK_a of 4.6 to generate the inactive low-pH form with Cu_H coordinated by M109, H107, and H172.

MATERIALS AND METHODS

All buffers and formic acid had a minimal purity of 99% and were acquired from Sigma-Aldrich. Dansyl-YVG was obtained from American Peptide Co. and the bovine liver catalase from Roche.

Expression and Purification of the PHMcc WT and M314H Mutant. The WT and M314H mutant catalytic cores were constructed as reported previously[21] and were isolated and purified from a Chinese hamster ovary (CHO) cell line as described previously.[25,26] The proteins were subjected to two cycles of dialysis for 8 h in 10 mM Tris-acetate buffer (WT at pH 8.4 and M314H at pH 8.2) and purified further on a BioCAD 700E Perfusion Chromatography Workstation (Applied Biosystems) by anion exchange on a 10 mm × 100 mm column packed with Poros 20 μm HQ anion exchange resin. The column was equilibrated with 5 column volumes of 10 mM Tris-acetate buffer at the appropriate pH, loaded with the partially purified enzyme, washed with 2 column volumes of buffer, and eluted with a 1 to 300 mM NaCl gradient over 10 column volumes. The fractions containing PHM were collected, pooled, and concentrated by ultrafiltration.

Determination of Copper and Protein Concentrations. The purified enzymes were reconstituted with cupric sulfate by slow addition of 2.5 molar equiv followed by exhaustive dialysis against 20 mM ultrapure sodium phosphate buffer (pH 8.0) containing 25 μM Cu(II) ion. The reconstituted enzyme was concentrated by ultrafiltration to approximately 4 mM in Cu(II) and used immediately. This protocol also served to reduce the level of exogenous chloride to levels that were insignificant relative to the protein copper concentration. Protein concentrations were determined using the OD_{280} on a Cary 50 spectrophotometer at ambient temperature using an extinction coefficient for a 0.1% solution at 280 nm of 0.980. Copper concentrations were determined using a Perkin-Elmer Optima 2000 DV inductively coupled plasma optical emission spectrometer.

Combination Buffer. The following buffers were mixed at 50 mM each and brought to the appropriate pH[3−10] using sodium hydroxide: *N*-cyclohexyl-2-aminoethanesulfonic acid (CHES), 4-(2-hydroxyethyl)-1-piperazineethanesulfonic acid (HEPES), 2-(*N*-morpholino)ethanesulfonic acid (MES), and formic acid.

High-Performance Liquid Chromatography (HPLC) Separation and Detection of Substrate and Product. Reverse-phase HPLC was performed with a Varian Pro Star solvent delivery module equipped with a Varian Pro Star model 410 autosampler (250 μL syringe, 100 μL sample loop) on a 250 mm × 4.6 mm Varian Microsorb-MV 100-5 C18 column. Substrate (dansyl-YVG, American Peptide Co.) and product (produced by the PHM-catalyzed reaction) were monitored by their dansyl fluorescence using a Waters 474 scanning fluorescence detector (λ_{ex} = 365 nm, and λ_{em} = 558 nm). Solvent A was 0.1% trifluoroacetic acid in water, and solvent B

was 0.1% trifluoroacetic acid in acetonitrile. Product was separated from substrate via isocratic loading and elution at 25% B in A.

Rates of reactions were determined by monitoring the rate of disappearance of substrate as a function of reaction time. A water-jacketed glass reaction vessel at 37 °C was used to perform the reaction. Two milliliters of combination buffer at varying pH values was introduced into the vessel followed by other reaction components at the following final concentrations: Cu(II) as copper sulfate (5 μM), catalase (26000 units), ascorbate (10 mM), and dansyl-YVG (variable concentrations between 5 and 400 μM). The reagents were incubated for at least 2 min to ensure thorough mixing. The reaction was initiated by addition of enzyme (0.05−0.80 μM). In a typical experiment, depending on the pH, 300 μL aliquots were removed every 30 s and placed in a 1.5 mL microcentrifuge tube containing 20 μL of 20% TFA to quench the reaction. Reactions at very low or very high pH values required longer sampling times because of slower reaction rates. Aliquots were then analyzed by HPLC to separate substrate and product, and the concentration of substrate remaining at each time point was determined by reference to a standard curve. Simulation of the rate data was performed by nonlinear regression, fitting the data to a model that assumes up to four enzyme species connected by deprotonation equilibria. Full details of the derivation and simulation of this model have been described in a previous publication.[24]

O_2 Electrode Activity Assays. Measurement of the rate of oxygen consumption was performed using a Rank Brother's oxygen electrode at 37 °C. Each reaction was performed in a total volume of 2 mL in the presence of catalase (amount determined empirically to suppress the rate of nonenzymatic oxygen consumption), ascorbate (10 μM), and Cu^{2+} as copper sulfate (5 μM), using 5, 10, 15, or 20 μL of a 10 μM PHM solution. Once reagents were added, the electrode was capped, and the reaction was initiated by addition of substrate to a maximal concentration of 400 μM using a Hamilton syringe.

Sample Preparation for XAS. All solutions were first made anaerobic, and all manipulations were conducted in the anaerobic chamber. Samples of the reduced WT enzyme were prepared in a single step by dilution of a 20 μL volume of 2 mM oxidized PHM [4 mM in Cu(II), 20 mM sodium phosphate (pH 8.0)], with 80 μL of the appropriate chloride-free combination buffer containing 5 mM ascorbate and 25% ethylene glycol. In one series of experiments to determine the effect of ascorbate on the EXAFS spectra, 1 mM ascorbate was used in place of 5 mM ascorbate. The sample was transferred to the XAS cuvette and flash-frozen by rapid immersion in liquid nitrogen. Samples of the M314H variant were prepared in an identical manner.

XAS Data Collection and Analysis. Cu K-edge (8980 eV) extended X-ray absorption fine structure (EXAFS) and X-ray absorption near edge structure (XANES) data were collected at the Stanford Synchrotron Radiation Lightsource at 3 GeV with currents between 100 and 80 mA on beamlines 7.3 and 9-3. The beamlines were configured with a liquid nitrogen-cooled Si[220] monochromator and a Rh-coated mirror upstream of the monochromator with a 13 keV energy cutoff to reject harmonics. On beamline 9.3, a second Rh mirror downstream of the monochromator was used to focus the beam. Data were collected in fluorescence mode using a high-count rate Canberra 30-element Ge array detector with maximal count rates of <120 kHz. A Z-1 metal (nickel) oxide filter and Soller slit assembly were placed in front of the detector to reduce the elastic scatter peak. Six to nine scans of a sample containing only sample buffer were collected, averaged, and subtracted from the averaged data for the protein samples to remove Z-1 K_β fluorescence and produce a flat pre-edge baseline. The samples (80 μL) were measured as aqueous glasses in 25% ethylene glycol at 15 K. Energy calibration was achieved by reference to the first inflection point of a copper foil (8980.3 eV) placed between the second and third ionization chambers. Data reduction and background subtraction were performed with the program modules of EXAFSPAK.[27] Data from each detector channel were inspected for glitches or dropouts before inclusion in the final average. Spectral simulation was conducted with EXCURVE version 9.2,[28−31] as previously described.[23] This allowed for inclusion of multiple scattering pathways between the metal center and the atoms of imidazole rings of the histidine residues. The experimental threshold energy, E_0, was chosen as 8985 eV. The structural parameters refined during the fitting process included coordination numbers (N), bond distances (R), and Debye−Waller factors ($2\sigma^2$), which result from both thermal motion and static disorder of the absorber−scatter pairs. The nonstructural parameter, ΔE_0, equivalent to a small correction to the threshold energy, was also allowed to vary but was restricted to a common value for every component in a given fit.

RESULTS

pH Dependence of the WT Protein. In previous work, we showed that in a mixed buffer system comprising acetate, HEPES, and CHES (50 mM each), the maximal PHM activity occurred at pH 7.0. The activity profile could be simulated by a model that assumed interconversion of an inactive protonated form and an active deprotonated form with a pK_a of 5.8. The interconversion exactly tracked a structural transition that can be observed by EXAFS, in which a Cu−S interaction assigned to a Cu(I)−S(Met) interaction decreased in intensity over a pH range indicative of an identical pK_a. This Cu−S interaction was tentatively assigned to the catalytically essential M314 ligand to Cu_M, where the decrease in intensity was interpreted as a change from a rigid (inactive) species with a small Debye−Waller factor to a highly flexible (active) species, and it was suggested that the highly flexible or fluxional Cu−S(Met) interaction was important for modulating the dynamics of H-atom tunneling during the H-atom abstraction step of the mechanism. However, it was noted that the EXAFS data could also be interpreted by the coordination of a second Cu−S(Met) species at low pH, although no clues about the identity of this second inactive species could be inferred. Interpretation of the data was further complicated by the fact that acetate buffer both inhibited the enzyme and shifted the pH maximum to 7.0 from its usual position of 5.8. When the experiment was performed in a MES/HEPES/CHES buffer mix, the pH maximum shifted back to its native value, but the buffering range of MES permitted data to be collected to only pH 5.0. This was sufficient to show that the pK_a for the Cu−S transition was also downshifted but insufficient to show that it fully tracked the catalytic activity under native conditions. Therefore, we developed a new buffer system in which formate was substituted for acetate, which activated rather than inhibited the enzyme and preserved the native pH optimum of 5.8. Using this system, we measured the EXAFS spectra of the ascorbate-

reduced enzyme and compared the pH dependence of the Cu−S "on" to "off" transition with the pH−activity profile.

Figure 2 shows the pH dependence of the Fourier transforms from pH 3 to 8 where it can be seen that the intense feature

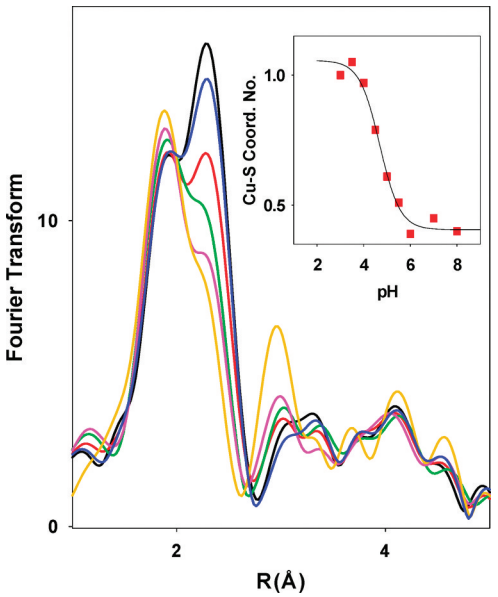

Figure 2. Fourier transforms of X-ray absorption data for WT PHMcc between pH 3 and 8. Spectra correspond to the pH values (from bottom to top) of 3.5, 4.0, 4.5, 5.0, 5.5, and 7.0. The inset shows the change in the shell occupancy of the Cu−S interaction (simulated using parameters listed in Table S1 of the Supporting Information) plotted as a function of pH and simulated using a pK_a of 4.69.

due to Cu−S scattering around 2.25 Å at low pH weakens to a shoulder between pH 5 and 7 and thereafter remains constant. These EXAFS data were fitted using (a) a previously validated structural model involving a mixed Cu−His and Cu−S coordination environment and (b) a simpler model involving a single shell of Cu−His and Cu−S scattering. At pH 7, the best fit to the data using a split shell model required 0.5 Cu−S at 2.24 Å, 1 Cu−N(His) at 1.85 Å, and 1 Cu−N(His) at 1.96 Å, which reflected a chemical model in which the two active site Cu centers were refined as separate shells (least-squares fitting parameter $F = 0.361$). This analysis has been discussed in detail in previous communications and is interpreted in terms of a three-coordinate $(His)_2S(Met)$ M site with an R_{Cu-His} of 1.96 Å and a two-coordinate $(His)_2$ H site with an R_{Cu-His} of 1.85 Å. However, although the split shell model generally gives better fits as measured by the value of the fitting parameter F, it is probably not justified by the resolution of the data ($k = 2-13$), where the minimal significant splitting of shells $\Delta R = \pi/2\Delta k = 0.14$ Å. Using a single shell of Cu−His scatterers, a comparable fit ($F = 0.373$) was obtained with 2.5 Cu−His at 1.95 Å and 0.5 Cu−S at 2.24 Å. It may be suggested that this fit is more representative of the reduced form of the native PHM because it accounts for all five of the His ligands, but the data do not easily distinguish between them. Therefore, the simpler single Cu−His shell fit was used throughout the analysis.

Simulation of EXAFS and FT data at pH 3.5 shows an increase in the shell occupancy of the Cu−S component from 0.5 to 1.0 and a slight lengthening of the Cu−S bond from 2.24 to 2.27 Å. The Cu−N(His) shell increases from 1.92 to 1.95 Å. Simulations for all pH values are compared with experimental data in Figures S1 and S2 of the Supporting Information with metrical details for each pH listed in Table S1 of the Supporting Information. The inset of Figure 2 shows the pH dependence of the Cu−S intensity, where the increased intensity has been simulated by keeping the Debye−Waller term constant at 0.010 Å^2 and refining the coordination number of the Cu−S shell. The latter increases from 0.45 ± 0.1 at pH 8 to 1.0 ± 0.1 at pH 3, following a titration curve with a pK_a of 4.69 ± 0.1.

Figure 3a shows the pH−activity profile (under saturating conditions of dansyl-YVG, ascorbate, and atmospheric oxygen)

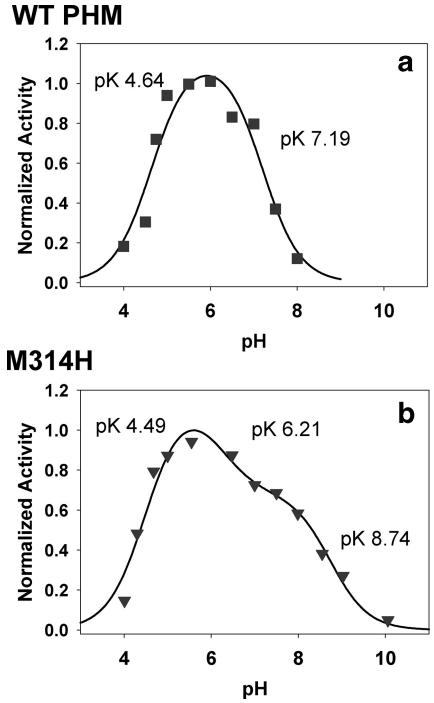

Figure 3. Normalized activity−pH profiles for (a) the WT and (b) M314H variant of PHM. Squares show experimental data, and black lines show simulated data. Activity data were measured using an O_2 electrode under saturating conditions of dansyl-YVG, ascorbate, and atmospheric oxygen. Activity data were normalized for ease of comparison. The data were analyzed as described previously,[24] in terms of an inactive species S1 present at low pH that is transformed into active state S2 (or active states S2 and S3 in the M314H variant) by deprotonantion steps with pK_a values as shown.

in a formate/MES/HEPES/CHES mixed buffer system that provides buffering capacity between pH 2.5 and 10. The profile can be simulated by assuming a single active species that is formed by deprotonation of an inactive precursor in a step with a pK_a of 4.64 ± 0.14 and is converted to an inactive state by a further deprotonation event with pK_a of 7.20 ± 0.15. The pH of the activity maximum (5.8) is identical to that obtained in 100 mM MES with no additional components, the buffer commonly used for measuring PHM activity. The pK_a of the activation phase is identical within experimental error to that obtained from EXAFS for Cu−S structural change.

The absorption edge of the WT PHM shows a feature at 8983 eV assigned to a 1s → 4p transition, the intensity of which can often be used as an indicator of coordination number. Two-coordinate complexes exhibit intense features associated with allowed 1s → $4p_{x,y}$ transitions, whereas the intensity is attenuated in three-coordinate systems because of mixing of s character into the excited state. Cu−S coordination also has the

dx.doi.org/10.1021/bi201193j | *Biochemistry* 2011, 50, 10819−10828

effect of decreasing the intensity due to increased covalency and consequent mixing of metal and ligand orbitals, such that the excited state no longer has pure p character. Inspection of Figure 4a shows that the intensity of the 8983 eV peak

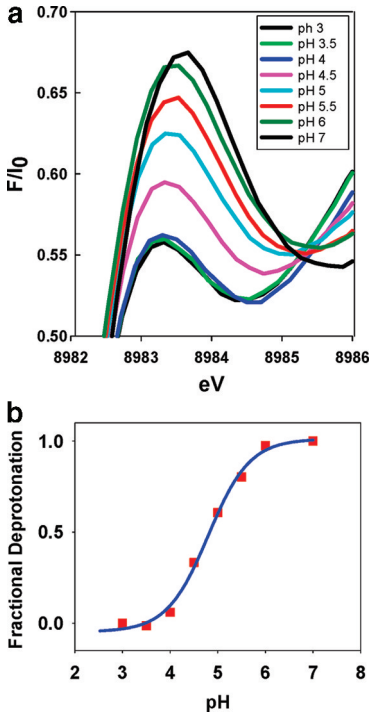

Figure 4. (a) pH dependence of the 1s → 4p transition on the absorption edge of WT PHMcc. (b) Fractional change in 8983 eV intensity (red squares) fitted to a pH titration curve with a pK_a of 4.8.

decreases with a decrease in pH, suggesting that the formation of the low-pH species is accompanied by an increase in the average coordination number of the two copper centers. Figure 4b shows a fit to the 8983 eV intensity data assuming that the changes are driven by a single deprotonation event. The calculated pK_a is 4.8 ± 0.1, which again matches the pK_a values of both the Cu−S structural transition and the enzyme activation. We conclude that the structural transition from high to low pH is accompanied by an increase in average coordination number at one or both Cu centers or alternatively or additionally involves an increase in covalency. The changes observed on the absorption edge are thus fully consistent with the conclusions from EXAFS analysis that a new species is formed at low pH with a strengthened Cu−S interaction and/or increased Cu−S coordination number. The fact that this new species tracks the activation of the enzyme both under native conditions (this work) and in acetate when the activity profile is shifted by 1.2 units to a higher pH[24] provides strong evidence that it is responsible for catalytic activation of the enzyme.

The S donor residue responsible for the Cu−S on to off transition is not immediately obvious, but two possibilities exist. First, as suggested previously, the catalytically essential M site ligand M314 could exist in two distinct conformations: an inactive strongly coordinated and rigidly bound on state that would result in an intense Cu−S interaction with a small DW factor and an active flexible or fluxional off state with correspondingly weaker bonding and higher DW. Second, at low pH, a structural transition initiated by protonation of a protein side chain could cause a second S donor ligand to coordinate at one of the copper centers. To probe these options, we constructed a PHM variant in which M314 was mutated to histidine. If the Cu−S transition originates from on to off states of M314, the prediction is that it should be eliminated in the M314H variant. Further, the pH dependence of M314H should be altered at low pH values.

Properties of the M314H Variant. The activity of the M314H variant was measured by following oxygen consumption using the O_2 electrode or by dansyl-YVG substrate depletion using HPLC. Table S2 of the Supporting Information compares K'_M for dansyl-YVG, k'_{cat}, and k'_{cat}/K'_M for WT and the M314H variant, where K'_M and k'_{cat} represent apparent kinetic constants measured under saturating ascorbate and

Table 1. Fits Obtained to the EXAFS of the M314H Variant of Peptidylglycine Monooxygenase

	Oxidized Proteins							
		Cu−N(His)[d]			Cu−O/N[e]			
	F[a]	No[b]	R (Å)[c]	DW (Å²)	No[b]	R (Å)[c]	DW (Å²)	$-E_0$
pH 7								
fit A	0.403	2.5	1.96	0.015	1.5	1.96[e]	0.015	5.20
fit B	0.478	3	1.97	0.014	1	1.96[e]	0.014	4.56
fit C	0.332	2.5	1.96	0.015	1.5	1.96[e]	0.015	
					0.5	2.33	0.006	4.98

	Reduced Proteins										
		Cu−N(His1)[d]			Cu−O/N			Cu−S			
	F[a]	No[b]	R (Å)[c]	DW (Å²)	No[b]	R (Å)[c]	DW (Å²)	No[b]	R (Å)[c]	DW (Å²)	$-E_0$
pH 7											
fit A	0.580	2.5	1.91	0.018	0.5	2.49	0.016				0.79
fit B	0.664	2.5	1.90	0.018							0.57
pH 3.5	0.543	2.0	1.90	0.017				0.5	2.25	0.007	0.92

[a] F is a least-squares fitting parameter defined by the equation $F^2 = (1/N)\sum_{i=1}^{N} k^6(\text{data} - \text{model})^2$. [b] Coordination numbers are generally considered accurate to ±25%. [c] In any one fit, the statistical error in bond lengths is ±0.005 Å. However, when errors caused by imperfect background subtraction, phase-shift calculations, and noise in the data are compounded, the actual error is probably closer to ±0.02 Å. [d] Fits modeled histidine coordination by an imidazole ring, which included single and multiple scattering contributions from the second-shell (C2/C5) and third-shell (C3/N4) atoms, respectively. The Cu−N−Cx angles were as follows: Cu−N−C2, 126°; Cu−N−C3, −126°; Cu−N−N4, 163°; Cu−N−C5, −163°. [e] First-shell distances of the Cu−N(His) and Cu−N/O (non-His) shells were constrained to be equal in fits to the oxidized proteins.

dx.doi.org/10.1021/bi201193j | *Biochemistry* 2011, 50, 10819–10828

atmospheric oxygen concentrations. Figure S3 of the Supporting Information compares the dansyl-YVG dependence of the steady-state rate for WT and M314H. Replacing M314 with His resulted in a decrease in k'_{cat} and an increase in K'_M, which were equivalent to a 96% decrease in the apparent k'_{cat}/K'_M. However, activity was not eliminated in the variant, indicating that the Met ligand was important but not essential for catalysis. Of further interest, although the catalytic rate was much reduced, the reaction remained 100% coupled as judged by stoichiometric conversion of oxygen and substrate into hydroxylated product. Figure 3b shows the normalized pH–activity profiles for the M314H variant (also measured under saturating concentrations of dansyl-YVG, ascorbate, and atmospheric oxygen) fitted to a model that assumed a number of states interconverting by proton dissociation steps. The profile differs from that of the WT in that at least four states appear to be present. At low pH, the variant is in inactive state S1 that converts to active state S2 with a pK_a of 4.49 ± 0.13, quite similar to that of the WT protein. Thereafter, a further deprotonation (pK_a = 6.21 ± 0.5) generates state S3, which also exhibits measurable activity and is further converted into inactive form S4 with a pK_a of 8.74 ± 0.20. It should be noted that because the total activity of S3 is much lower than that of WT, it could be present yet undetectable in the WT profile. Although differences exist in the high-pH range, we can conclude that the formation of the active S2 state appears to follow a pH profile similar to that of the WT.

Because Met 314 is coordinated in an axial position and cannot be detected by EXAFS in the oxidized form of the WT protein, the prediction is that substitution of Met with His should have no effect on the EXAFS spectrum of oxidized M314H. This prediction was borne out by the finding that the EXAFS spectrum of oxidized M314H could be simulated using a parameter set identical to that for the WT protein. These parameters are given for data collected at pH 7 in Table 1. The spectrum (Figure S4 of the Supporting Information) is simulated well by four low-Z scatterers at 1.96. In the WT protein, we showed previously that the fit was consistent with an average of 2.5 His ligands per Cu, with an additional 1.5 non-His (solvent) ligands completing the expected four-coordinate character in the equatorial plane.[23] For M314H, there is the additional possibility that His314 might replace a water/hydroxide ligand in the equatorial plane, and M314H oxidized fit B involving three His ligands at each copper (Table 1) shows that such a fit is only slightly worse as judged by the value of the goodness of fit parameter (F). The fit could be improved (~20%) by a model in which the additional His ligand was bound at a longer (axial) distance suggesting that His314 coordinates like its Met homologue. We also used XAS to investigate the coordinate structure of the Cu center of the reduced M314H variant at pH 7 and 3.5. We explored fits that either employed all low-Z scatterers [Cu–N(His) and additional O/N shells] or included heavier (Cu–S/Cl) scatterers. Figure 5a shows the EXAFS data for pH 7.0, which are best simulated with low-Z scatterers and no S/Cl component. The data fit best to 2.5 Cu–His at 1.91 Å and are somewhat improved (14%) by inclusion of an additional 0.5 low-Z scatterer at 2.5 Å, which would be consistent with the coordination of a third His ligand at Cu_M. However, the correlation between DW factors and coordination numbers generally prohibits estimation of shell occupancy to better than ~25%, so that it is difficult to detect the presence of one additional His ligand at Cu_M in either the oxidized or reduced form.

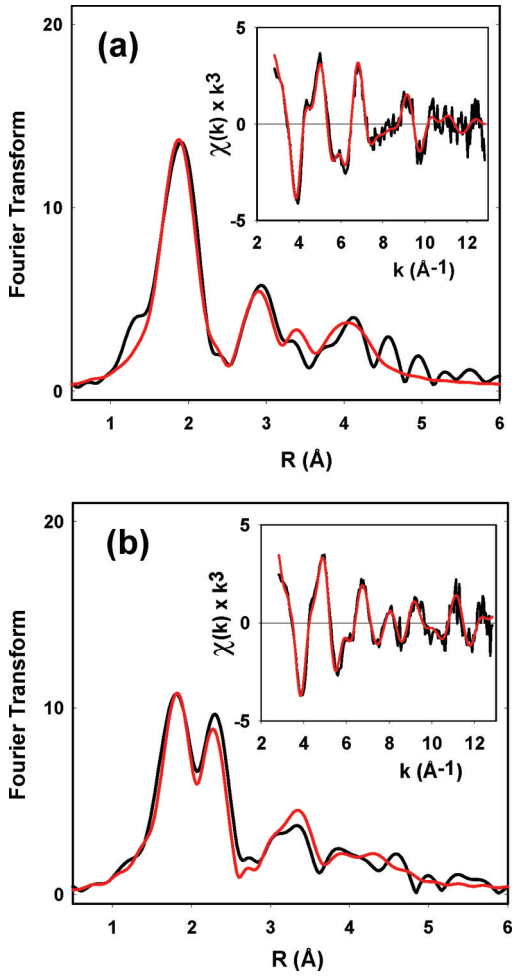

Figure 5. Experimental and simulated Fourier transforms and EXAFS (insets) for the reduced forms of the M314H variants at (a) pH 7 and (b) pH 3.5. Parameters used in the fits are listed in Table 1.

The EXAFS of M314H at pH 3.5 is shown in Figure 5b with parameters listed in Table 1. The data show a pattern similar to that observed for the WT protein, viz. strong scattering amplitude at ~2.2–2.3 Å that can be simulated by 0.5 Cu–S/Cl at 2.25 Å with a DW factor of 0.007 $Å^2$. This result establishes that this Cu–S interaction does not arise from a Met-on configuration of the active site M314 ligand and must arise from coordination of a different S donor ligand at low pH.

Absorption edges of the reduced M314H samples show 8983 eV peaks that are more intense than those of the WT at both high and low pH values (Figure 6). This supports the conclusion that His314 is probably dissociated from Cu_M.

The low-pH Cu–S/Cl scatterering could arise from coordination of S from cysteine or methionine or could be due to coordination of exogenous Cl. The latter possibility is unlikely because (a) the protein was isolated under conditions where exogenous chloride was minimized and (b) it is chemically unreasonable because HCl is a strong acid, and it is hard to envisage why Cl binding should be strongly influenced by deprotonation of a protein side chain. Cu–S(Cys) coordination is also unlikely because all 10 Cys residues in PHMcc form disulfide cross-links. The data notwithstanding, we considered the possibility that in the presence of 5 mM

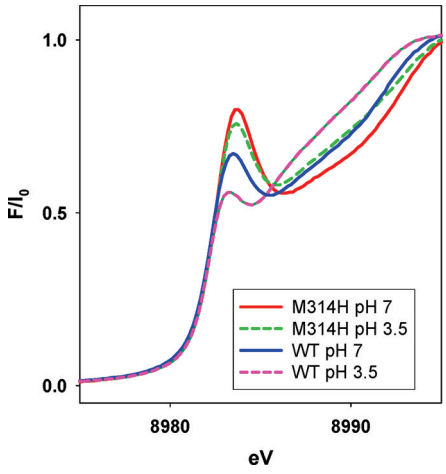

Figure 6. Comparison of the 1s → 4p absorption edge transition for WT and M314H PHMcc at pH 7 and 3.5.

ascorbate a disulfide cross-link might be reduced to a bis-thiol. C315 is an obvious candidate because it anchors the β-sheet that carries the M314 residue as well as the peptide substrate binding N316 and Y318.[9−12] To probe Cu−S(Cys) coordination, we compared the low-pH forms of a 1 mM sample of WT PHMcc reduced with 5 and 1 equiv of ascorbate and obtained identical EXAFS spectra with a fully coordinated Cu−S species (Figure S5 of the Supporting Information). Because all the reducing equivalents in the 1 mM ascorbate sample were required to reduce the two copper centers to Cu(I), we conclude that in this sample all disulfide cross-links must be intact. Therefore, the low-pH S donor must be a methionine residue.

DISCUSSION

We have shown that catalytic inactivation of PHM in the pH range of 8−3 is accompanied by a structural change between the two states of the protein, an active state with a single, weakly bound Cu−S interaction present at higher pH and an inactive state involving a significant increase in the coordination number or strength of the Cu−S interaction at lower pH values. We first reported this effect in an earlier paper where the activity was measured in acetate buffer, which shifted the activity maximum from its native value of pH 5.8 to 7, but we were unable to fully determine the titration profile under native conditions because of the inaccessibilty of pH value of <5 in MES buffer. In this work, we have extended the pH range downward using a formate buffer system and have been able to show that the Cu−S "off-to-on" structural transition still accurately tracks the inactivation of the enzyme in the pH 8−3 range. This extends our earlier study into the pH range relevant to the physiological state of the enzyme and confirms that the off state is the catalytically active form. The Cu−S interaction present in the off state has been assigned to the Cu−S(Met314),[7,23] where M314 is a ligand to the catalytic M site and is characterized by a larger than usual Debye−Waller factor relative to those of other Cu(I)−S interactions in Cu−Met$x$ or Cu−HisMet environments,[32−36] suggesting a highly dynamic or fluxional environment. Earlier, we suggested that such dynamics might couple into vibrational modes of the catalytic site that were critical for H-tunneling in H-atom abstraction from the substrate, and further that the on state might represent more rigid dynamics for Cu−Met314 interaction resulting in a loss of coupling into these critical tunneling modes.[24] However, two lines of evidence presented in the earlier study cast doubt on whether the on state was the result of a local conformational effect at the M site or arose from a more global conformational effect, perhaps involving changes at the H site. Specifically, photoreduction in the frozen state at low pH resulted in a loss of solvent coordination but failed to induce the on state, while the K_D for peptide substrate binding close to the M site was independent of pH. In this study, we tested these predictions in a variant in which the catalytic M314 residue was mutated to histidine and demonstrated that the off-to-on transition was still observed in the absence of Met 314. This has led to the evolution of the model in which we conclude that the origin of the strong Cu−S interaction at low pH cannot be a more tightly bound form of the M314 residue but must be an additional Cu−S interaction that binds at one of the two copper centers in the low-pH inactive form but dissociates at higher pH to form the catalytically active species.

In other work,[3] we have shown that a similar Cu−S on-to-off transition occurs in the homologous enzyme TBM, suggesting a functional role for the transition in setting the pH optimum of these enzymes around 5.5. This may be physiologically important because PHM, DBM, and TBM are each localized to secretory granules whose internal pH coincides with the pH optimum of the enzymes.[37] Sequence comparison of PHM, DBM, TBM, and MOX reveals four conserved cysteines and two conserved methionines. All four of the conserved Cys residues occur as disulfide cross-links in PHM and, to coordinate to Cu(I), would have to be reduced to thiols. It is possible that ascorbate at ∼5 mM (the concentration used to reduce the copper centers) might also reduce one or more of these disulfide cross-links, releasing a free thiol. For example, reduction of the cross-link between Cys315 and Cys293 would place a reduced thiol adjacent to the M site Met ligand M314. With this in mind, we compared EXAFS data of the low-pH ascorbate-reduced WT enzyme produced with 5-fold versus equimolar concentrations of ascorbate. The mechanism of reduction by ascorbate has been shown in DBM to proceed by one-electron redox to form the monodehydroascobate radical followed by disproportionation to form dehydroascorbate and regenerated ascorbate products.[38] Thus, 1 equiv of ascorbate is sufficient to reduce both copper centers but is insufficient to reduce additional disulfides. The experimental finding that the Cu−S intensity was identical in 5-fold and 1-fold ascorbate reduction experiments therefore allows us to rule out cysteine as the origin of the sulfur donor.

PHM, TBM, and DBM have two conserved Met residues, M314 and M109 (PHM numbering). M314 is the catalytic Met residue, and we have shown in this study that its mutation to histidine does not affect the intensity of the Cu−S feature at low pH. This suggests that M109 may be the S donor. In MOX, the residue is Ile, and interestingly, although the function is unknown, the protein is retained in the ER and does not appear to enter the secretory pathway. Consequently, it would have no need to adjust its pH optimum to 5 via a His to Met transition.[39] M109 is close to the H site (Figure 7) but extends away from the copper center on the same β-strand that holds the coordinated H108 and H107 ligands. Protonation of either H107 or H108 might induce rearrangement of this strand to coordinate the M109 thioether. However, of the additional 14 Met residues (excluding M314 and M109) identified in the PHMcc structure, two (M116 and M82) are in the vicinity of the H site and one (M208) is in the vicinity of the M site.

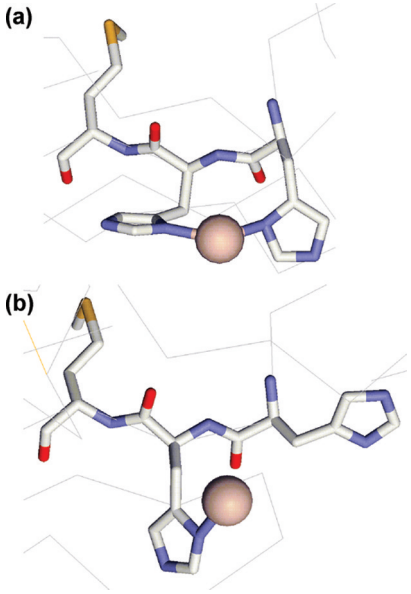

Figure 7. Structural depiction of two different conformations of the H center in PHMcc showing differences in the orientation of residues H107, H108, and M109. The H172 ligand has been omitted for the sake of clarity. (a) Conformation found in WT PHMcc (PDB entry 1OPM) with each His ligand coordinated by imidazole Nδ. (b) Conformation observed in the M314I variant (PDB entry 1YI9) with H107 dissociated.

Therefore, while the assignment of M109 is supported by available data, it must be considered as tentative at this time.

There is precedent for different conformational states at the H center. A crystal structure of the M314I variant showed an altered conformation, with H107 dissociated from the copper.[11] A comparison of this structure with that of the WT oxidized protein is shown in Figure 7. The WT structure indicates rather poor hybridization of the H107 Nδ donor atom, suggesting a strained conformation induced by the coordination of the contiguous H107 and H108 imidazole side chains that is relieved in the M314I structure by dissociation of H107. Protonation of H108 at low pH would be an alternative way to relieve this strain, generating the more stable M109-X-H107 coordination.

The pK_a for the catalytic transition is 4.6, within the range determined for protonation of histidine residues coordinated to Cu(I). Protonation and dissociation of a Cu(I)-bound imidazole residue occur in reduced forms of cupredoxins[40,41] and Cu/Zn superoxide dismutases.[42−44] The simultaneous addition of a proton along with an electron keeps the overall charge at the active site constant and in the case of cupredoxins has been ascribed to proton-coupled electron transfer. In cupredoxins, the C-terminal histidine ligand is contained within a short loop of structure located between the Cys and Met ligands, and variation of both the sequence and length of this loop has been shown to have profound effects on the value of the pK_a for histidine protonation. For example, replacement of the native loop of azurin (C^{112}TFPGH^{117}SALM, pK_a for H^{117} < 2) with shorter loops from amicyanin or plastocyanin produces chimeras with pK_a values for protonation of the corresponding histidine of 5.5 and 4.3, respectively. For plastocyanin, the pK_a values of the native protein and the chimera in which the native loop (C^{84}SPH^{87}QGAGM^{92}) is replaced with the azurin loop sequence are 4.7 and 4.9, respectively.[45] Taken together, the studies on cupredoxins have demonstrated sensitivity of Cu(I)-coordinated histidines to loop length, identity of non-coordinated residues within the loop, and second-shell effects such as solvation and H-bonding. Similar effects are likely to modulate the acidity of the Cu_H-coordinating histidine residues in PHM and provide a reasonable rationale for the observed pK_a value.

The apparent kinetic constants for the M314H variant indicate that the catalytic M314 has a complex role. The increase in K'_M implies that reversible binding events that precede the first irreversible catalytic step are altered in the mutant, while the decrease in k'_{cat} implies additional effects on the irreversible catalytic step. EXAFS studies confirm the loss of the catalytic Cu−S interaction at Cu_M but provide no evidence either way for coordination of the substituted His residue. The additional deprotonation step observed at high pH may indicate minor mechanistic differences, perhaps due to structural perturbations in the mutant. However, it is clear from this work that catalysis does occur in the His mutant, and product formation remains tightly coupled to oxygen consumption, suggesting that the mechanism remains essentially the same, albeit with a reduced catalytic efficiency. Therefore, M314 serves to increase catalytic efficiency rather than providing a unique mechanistic role. Further studies of additional methionine variants aimed at establishing the coordination of M109 (and/or other Met residues) and the mechanistic role of M314 are ongoing in our laboratory.

■ ASSOCIATED CONTENT

Supporting Information

Five figures and two tables. This material is available free of charge via the Internet at http://pubs.acs.org.

■ AUTHOR INFORMATION

Corresponding Author

*Phone: (503)748-1384. Fax: (503)748-1464. E-mail: ninian@comcast.net.

Present Address

[†]VLST Corp., 307 Westlake Ave. N., Suite 300, Seattle, WA 98109.

Funding

This work was supported by a grant from the National Institutes of Health (R01 NS027583 to N.J.B.).

■ ACKNOWLEDGMENTS

We thank Drs. Betty Eipper and Richard Mains for providing us with cell lines expressing the M314H variant. We gratefully acknowledge the use of facilities at the Stanford Synchrotron Radiation Lightsource, which is supported by the National Institutes of Health Biomedical Research and Technology Program Division of Research Resources and by the U.S. Department of Energy Office of Biological and Environmental Research.

■ ABBREVIATIONS

DBM, dopamine β-monooxygenase; DW, Debye−Waller factor; dansyl-YVG, dansyl-tyrosylvalylglycine; EXAFS, extended X-ray absorption fine structure; FT, Fourier transform; PDB, Protein Data Bank; PHM, peptidylglycine monooxygenase; TBM, tyramine β-monooxygenase; XANES, X-ray absorption near-edge structure; XAS, X-ray absorption spectroscopy.

REFERENCES

(1) Prigge, S. T., Mains, R. E., Eipper, B. A., and Amzel, L. M. (2000) New insights into copper monooxygenases and peptide amidation: Structure, mechanism and function. *Cell. Mol. Life Sci. 57*, 1236−1259.

(2) Klinman, J. P. (2006) The copper-enzyme family of dopamine β-monooxygenase and peptidylglycine α-hydroxylating monooxygenase: Resolving the chemical pathway for substrate hydroxylation. *J. Biol. Chem. 281*, 3013−3016.

(3) Hess, C. R., Klinman, J. P., and Blackburn, N. J. (2010) The copper centers of tyramine β-monooxygenase and its catalytic-site methionine variants: An X-ray absorption study. *J. Biol. Inorg. Chem. 15*, 1195−1207.

(4) Hess, C. R., Wu, Z., Ng, A., Gray, E. E., McGuirl, M. A., and Klinman, J. P. (2008) Hydroxylase activity of Met471Cys tyramine β-monooxygenase. *J. Am. Chem. Soc. 130*, 11939−11944.

(5) Blackburn, N. J., Hasnain, S. S., Pettingill, T. M., and Strange, R. W. (1991) Copper K-EXAFS studies of oxidized and reduced dopamine-β-hydroxylase: Confirmation of a sulfur ligand to Cu(I) in the reduced enzyme. *J. Biol. Chem. 266*, 23120−23127.

(6) Pettingill, T. M., Strange, R. W., and Blackburn, N. J. (1991) Carbonmonoxy dopamine-β-hydroxylase: Structural characterization by FTIR, fluorescence and XAS spectroscopy. *J. Biol. Chem. 266*, 16996−17003.

(7) Boswell, J. S., Reedy, B. J., Kulathila, R., Merkler, D. J., and Blackburn, N. J. (1996) Structural investigations on the coordination environment of the active-site copper centers of recombinant bifunctional peptidylglycine α-amidating enzyme. *Biochemistry 35*, 12241−12250.

(8) Chen, P., Bell, J., Eipper, B. A., and Solomon, E. I. (2004) Oxygen activation by the noncoupled binuclear copper site in peptidylglycine α-hydroxylating monooxygenase. Spectroscopic definition of the resting sites and the putative $CuII_M$-OOH intermediate. *Biochemistry 43*, 5735−5747.

(9) Prigge, S. T., Kolhekar, A. S., Eipper, B. A., Mains, R. E., and Amzel, L. M. (1997) Amidation of bioactive peptides: The structure of peptidylglycine α-hydroxylating monooxygenase. *Science 278*, 1300−1305.

(10) Prigge, S. T., Kolhekar, A. S., Eipper, B. A., Mains, R. E., and Amzel, L. M. (1999) Substrate-mediated electron transfer in peptidylglycine α-hydroxylating monooxygenase. *Nat. Struct. Biol. 6*, 976−983.

(11) Siebert, X., Eipper, B. A., Mains, R. E., Prigge, S. T., Blackburn, N. J., and Amzel, L. M. (2005) The catalytic copper of peptidylglycine α-hydroxylating monooxygenase also plays a critical structural role. *Biophys. J. 89*, 3312−3319.

(12) Chufan, E. E., Prigge, S. T., Siebert, X., Eipper, B. A., Mains, R. E., and Amzel, L. M. (2010) Differential reactivity between two copper sites in peptidylglycine α-hydroxylating monooxygenase. *J. Am. Chem. Soc. 132*, 15565−15572.

(13) Magnus, K. A., Hazes, B., Ton-That, H., Bonaventura, C., Bonaventura, J., and Hol, W. G. J. (1994) Crystallographic analysis of oxygenated and deoxygenated states of arthropod hemocyanin shows unusual differences. *Proteins: Struct., Funct., Genet. 19*, 302−309.

(14) Gerdemann, C., Eicken, C., and Krebs, B. (2002) The crystal structure of catechol oxidase: New insight into the function of type-3 copper proteins. *Acc. Chem. Res. 35*, 183−191.

(15) Chen, P., and Solomon, E. I. (2004) O_2 activation by binuclear Cu sites: Noncoupled versus exchange coupled reaction mechanisms. *Proc. Natl. Acad. Sci. U.S.A. 101*, 13105−13110.

(16) Matoba, Y., Kumagai, T., Yamamoto, A., Yoshitsu, H., and Sugiyama, M. (2006) Crystallographic evidence that the dinuclear copper center of tyrosinase is flexible during catalysis. *J. Biol. Chem. 281*, 8981−8990.

(17) Lewis, E. A., and Tolman, W. B. (2004) Reactivity of dioxygen-copper systems. *Chem. Rev. 104*, 1047−1076.

(18) Evans, J. P., Ahn, K., and Klinman, J. P. (2003) Evidence that dioxygen and substrate activation are tightly coupled in dopamine β-monooxygenase: Implications for oxygen activation. *J. Biol. Chem. 278*, 49691−49698.

(19) Bauman, A. T., Yukl, E. T., Alkevich, K., McCormack, A. L., and Blackburn, N. J. (2006) The hydrogen peroxide reactivity of peptidylglycine monooxygenase supports a Cu(II)-superoxo catalytic intermediate. *J. Biol. Chem. 281*, 4190−4198.

(20) Chen, P., and Solomon, E. I. (2004) Oxygen activation by the noncoupled binuclear copper site in peptidylglycine α-hydroxylating monooxygenase. Reaction mechanism and role of the noncoupled nature of the active site. *J. Am. Chem. Soc. 126*, 4991−5000.

(21) Eipper, B. A., Quon, A. S. W., Mains, R. E., Boswell, J. S., and Blackburn, N. J. (1995) The catalytic core of peptidylglycine α-hydroxylating monooxygenase: Investigation by site-directed mutagenesis, Cu X-ray absorption spectroscopy, and electron paramagnetic resonance. *Biochemistry 34*, 2857−2865.

(22) Kolhekar, A. S., Keutman, H. T., Mains, R. E., Quon, A. S. W., and Eipper, B. A. (1997) Peptidylglycine α-hydroxylating monooxygenase: Active site residues, disulfide linkages, and a two-domain model of the catalytuc core. *Biochemistry 36*, 10901−10909.

(23) Blackburn, N. J., Rhames, F. C., Ralle, M., and Jaron, S. (2000) Major changes in copper coordination accompany reduction of peptidylglycine monooxygenase. *J. Biol. Inorg. Chem. 5*, 341−353.

(24) Bauman, A. T., Jaron, S., Yukl, E. T., Burchfiel, J. R., and Blackburn, N. (2006) pH dependence of peptidylglycine monooxygenase. Mechanistic implications for Cu-methionine binding dynamics. *Biochemistry 45*, 11140−11150.

(25) Jaron, S., and Blackburn, N. J. (1999) Does superoxide channel between the copper centers in peptidylglycine monooxygenase? A new mechanism based on carbon monoxide reactivity. *Biochemistry 38*, 15086−15096.

(26) Bauman, A. T., Ralle, M., and Blackburn, N. (2007) Large scale production of the copper enzyme peptidylglycine monooxygenase using an automated bioreactor. *Protein Expression Purif. 51*, 34−38.

(27) George, G. N. (1990) EXAFSPAK; Stanford Synchrotron Radiation Laboratory, Menlo Park, CA.

(28) Binsted, N., Gurman, S. J., and Campbell, J. W. (1998) EXCURV9.2; Daresbury Laboratory, Warrington, England.

(29) Gurman, S. J., Binsted, N., and Ross, I. (1984) A rapid, exact, curved-wave theory for EXAFS calculations. *J. Phys. C: Solid State Phys. 17*, 143−151.

(30) Gurman, S. J., Binsted, N., and Ross, I. (1986) A rapid, exact, curved-wave theory for EXAFS calculations. II. The multiple-scattering contributions. *J. Phys. C: Solid State Phys. 19*, 1845−1861.

(31) Binsted, N., and Hasnain, S. S. (1996) State of the art analysis of whole X-ray absorption spectra. *J. Synchrotron Radiat. 3*, 185−196.

(32) Loftin, I. R., Franke, S., Blackburn, N. J., and McEvoy, M. M. (2007) Unusual Cu(I)/Ag(I) coordination of *Escherichia coli* CusF as revealed by atomic resolution crystallography and X-ray absorption spectroscopy. *Protein Sci. 16*, 2287−2293.

(33) Loftin, I. R., Blackburn, N. J., and McEvoy, M. M. (2009) Tryptophan Cu(I)-π interaction fine-tunes the metal binding properties of the bacterial metallochaperone CusF. *J. Biol. Inorg. Chem. 14*, 905−912.

(34) Bagai, I., Liu, W., Rensing, C., Blackburn, N. J., and McEvoy, M. M. (2007) Substrate-linked conformational change in the periplasmic component of a Cu(I)/Ag(I) efflux system. *J. Biol. Chem. 282*, 35695−35702.

(35) Sarret, G., Favier, A., Coves, J., Hazemann, J. L., Mergeay, M., and Bersch, B. (2010) CopK from *Cupriavidus metallidurans* CH34 binds Cu(I) in a tetrathioether site: Characterization by X-ray absorption and NMR spectroscopy. *J. Am. Chem. Soc. 132*, 3770−3777.

(36) Rubino, J. T., Riggs-Gelasco, P., and Franz, K. J. (2010) Methionine motifs of copper transport proteins provide general and flexible thioether-only binding sites for Cu(I) and Ag(I). *J. Biol. Inorg. Chem. 15*, 1033−1049.

(37) Wu, M. M., Grabe, M., Adams, S., Tsien, R. Y., Moore, H. P., and Machen, T. E. (2001) Mechanisms of pH regulation in the regulated secretory pathway. *J. Biol. Chem. 276*, 33027−33035.

(38) Diliberto, E. J. Jr., and Allen, P. L. (1981) Mechanism of dopamine β-hydroxylation. Semidehydroascorbate as the enzyme oxidation product of ascorbate. *J. Biol. Chem. 256*, 3385−3393.

(39) Xin, X., Mains, R. E., and Eipper, B. A. (2004) Monooxygenase X, a member of the copper-dependent monooxygenase family localized to the endoplasmic reticulum. *J. Biol. Chem. 279*, 48159−48167.
(40) Guss, J. M., Harrowell, P. R., Murata, M., Norris, V. A., and Freeman, H. C. (1986) Crystal structure analyses of reduced (CuI) poplar plastocyanin at six pH values. *J. Mol. Biol. 192*, 361−387.
(41) Li, C., Sato, K., Monari, S., Salard, I., Sola, M., Banfield, M. J., and Dennison, C. (2011) Metal-binding loop length is a determinant of the pKa of a histidine ligand at a type 1 copper site. *Inorg. Chem. 50*, 482−488.
(42) Bertini, I., Luchinat, C., and Monnanni, R. (1985) Evidence of the breaking of the copper-imidazolate bridge in copper/cobalt-substituted superoxide dismutase upon reduction of the Cu(II) centers. *J. Am. Chem. Soc. 107*, 2178−2179.
(43) Blackburn, N. J., Hasnain, S. S., Binsted, N., Diakun, G. P., Garner, C. D., and Knowles, P. F. (1984) An extended-X-ray-absorption-fine-structure study of bovine erythrocyte superoxide dismutase in aqueous solution. Direct evidence for three-coordinate Cu(I) in the reduced enzyme. *Biochem. J. 219*, 985−990.
(44) Banci, L., Bertini, I., Cramaro, F., Del Conte, R., and Viezzoli, M. S. (2002) The solution structure of reduced dimeric copper zinc superoxide dismutase. The structural effects of dimerization. *Eur. J. Biochem. 269*, 1905−1915.
(45) Li, C., Banfield, M. J., and Dennison, C. (2007) Engineering copper sites in proteins: Loops confer native structures and properties to chimeric cupredoxins. *J. Am. Chem. Soc. 129*, 709−718.